NC STATE UNIVERSITY

College of Engineering

Department of Mechanical and Aerospace Engineering

MAE-315, Section 002

Dynamics of Machines

Project #1

Landing Gear Design Project

Written By: Group 18

Group 18 Members: **John Peterson**
Maia Judd
Thomas Teeters

Project Submission Deadline: **03/23/2022**

Abstract

The purpose of this project is to inspect the current design of an airplane's landing gear and find out how to improve it. It is impossible to improve the landing gear in every way without it losing some efficiency in another category. In this case, design improvements need to be made in specific areas with the intent of improving the design at the speed the airplane will land at, where the landing gear is needed most.

The best way to see the changes made to the design of the landing gear is to plot the magnitude of the amplitude of the landing gear vs. the frequency of the system. The frequency that corelates to the speed of the airplane as it is landing is determined to be around 30 rad/s. The amplitude of the new designs needs to fall below .145 m at the 30 rad/s frequency value. The landing gear consisted of a spring and a damper so these values could either increase or decrease to improve the system. When the spring constant value is increased, the peak on the amplitude graph shifts to the right and shifts left when the spring constant value is decreased. Likewise, when the damping constant is increased or decreased, the amplitude peak will shift down or up respectively.

Since there is not a design that will be better than all others in every category, 3 potential designs are needed that all meet the criteria of the amplitude magnitude remaining below .145 m at 30 rad/s. With 3 reasonable designs ready, the next step is to determine which is the best option for the landing gear. This is done by evaluating the designs based on how well they function, the feasibility of the designs, and how available resources are for the designs.

Although all 3 of the potential designs had commercially available springs and would therefore be economically viable options, 2 of the designs would make the landing gear too bulky which would decrease the usable space for storage and seating. The design that proved to be the most practical and was ultimately selected was not only much more compact but also had a higher damping constant which would provide a soother landing for the airplane and improve the comfort of the passengers.

With a design selected, the next test was to see how the design holds up over an unforeseen change in the runway surface. This is done using the Fourier expansion formula to evaluate what frequency value of the design might be an issue by comparing the frequency produced by the motion over the unforeseen change in the runway to the natural frequency of the landing gear system.

1. Problem Formulation

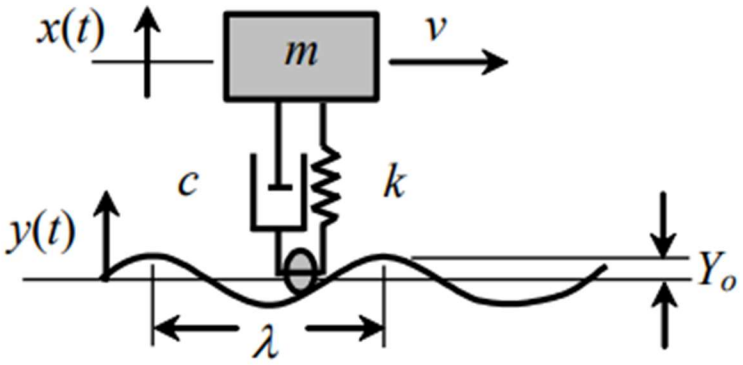

Figure 1, Picture of the Given Model

This is a simplified view of an airplane's landing gear as it travels over a landing surface. The runway landing surface's motion can be described by the function y(t). The function x(t) describes the vertical motion from the static equilibrium position as it travels over the runway surface. The wavelength of the runway is 12m, the runway surface amplitude is described by Y_o, and the velocity of the landing gear is to the right of the figure. The mass of the object is given as m = 2000 kg and the spring and damper constants are noted in the figure by k and c respectively.

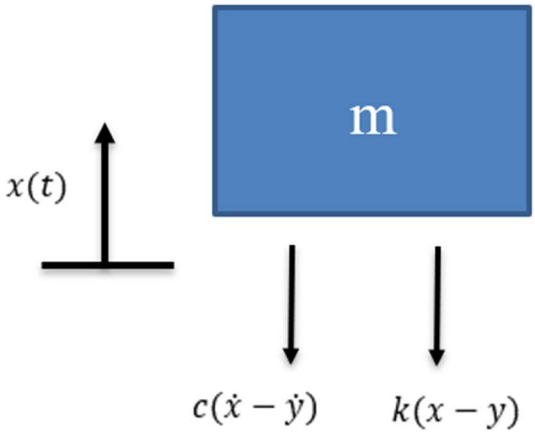

Figure 2, Free Body Diagram

From the free body diagram, Newtons 2nd Law can be used to derive the Equations of Motion (EOM).

$$m\ddot{x} + c\dot{x} + kx = c\dot{y} + ky, \text{ where } y(t) = Y_0\cos(\omega t)$$

From the EOM, the particular solution $x_p(t)$ can then be derived. Only the final form is shown below but the whole derivation is explained in Appendix B.

$$x_p(t) = |\tilde{X}|e^{i(\omega t - \phi)} \text{ where } |\tilde{X}| \text{ and } \phi \text{ are given by}$$

$$|\tilde{X}| = Y_0 \left| \sqrt{\frac{(k)^2 + (c\omega)^2}{(k - m\omega^2)^2 + (c\omega)^2}} \right|$$

$$\phi = \tan^{-1} \frac{cm\omega^3}{k(k - m\omega^2) + (c\omega)^2}$$

Periodic Force EOM and Steady State Response

Using the given square wave surface, a Fourier series can be used to approximate the corresponding function, external to the system. Because this computed y(t), shown below, takes the same form as the original external function, the computed particular solution looks very similar to the last particular solution. Now, replacing Y_0 is the constant b_j and replacing ω is the combination of $j\omega_0$. However, unlike the last response, there is also now an infinite series of contributing values where j is any odd integer instead of just two terms. The Fourier series approximation, EOM, and particular solution are all shown below and the complete derivation along with the graph of the square wave can all be found in appendix C.

$$y(t) \cong \sum_{j=1,3,5}^{\infty} \frac{4A}{j\pi} \sin j\omega_0 t$$

$$m\ddot{x} + c\dot{x} + kx = c \sum_{j=1,3,5}^{\infty} ij\omega_0 b_j e^{ij\omega_0 t} + k \sum_{j=1,3,5}^{\infty} b_j e^{ij\omega_0 t}$$

$$x_p(t) = \sum_{j=1,3,5}^{\infty} |\tilde{X}_j| e^{i(j\omega_0 t - \phi_j)}$$

$$|\tilde{X}_j| = b_j \left| \sqrt{\frac{(k)^2 + (cj\omega_0)^2}{(k - m(j\omega_0)^2)^2 + (cj\omega_0)^2}} \right|$$

$$\phi_j = \tan^{-1} \frac{cm(j\omega_0)^3}{k(k - m(j\omega_0)^2) + (cj\omega_0)^2}$$

where $b_j = \frac{4A}{j\pi}$

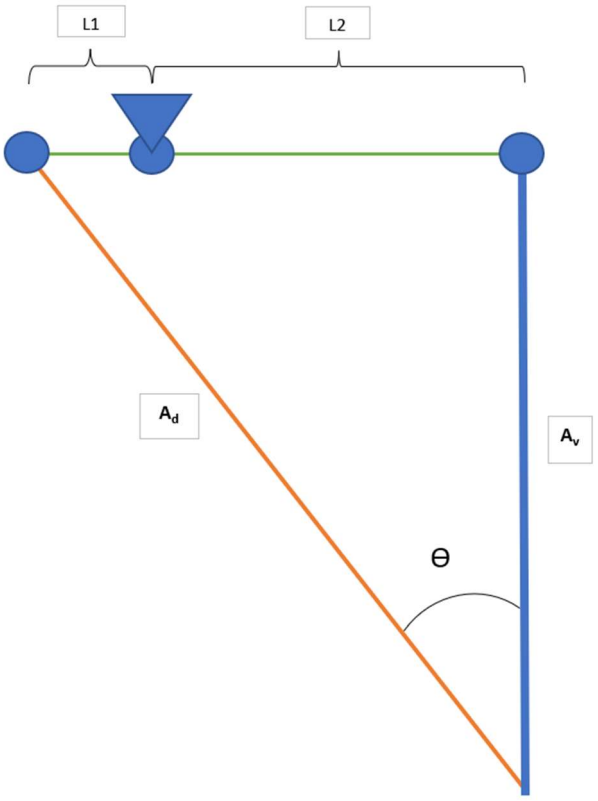

Figure 3, Orientation of Vertical and Diagonal Springs

This diagram represents the orientation of the springs in our design. Each design option evaluated involves a single vertical spring which is surrounded by several diagonal springs (Figure 8, Figure 9, and Figure 10). Each diagonal spring (Ad shown in orange in Figure 3) is connected to the vertical spring (Av shown in blue above) by two links L1 and L2 (shown in green in Figure 3). Using a ratio of the links where the length of L2 is greater than L1, we can reduce the amplitude of the motion of the diagonal spring relative to the amplitude of the vertical spring, which experiences the total movement of the wheels in the landing gear. In commercially available springs, as amplitude or travel of the spring is increased, the maximum k value is reduced. By reducing the travel of the diagonal spring, larger k value springs can be selected to meet the design requirements for the landing gear while still allowing the landing gear to travel the required amplitude. While the vertical spring is fully contributing to the k value of the system, only the cosine component of the theta angle of the diagonal springs (Figure 3) will contribute to the k value.

θ = angle between the vertical and diagonal springs

$$R = \frac{L_2}{L_1} = Link\ Ratio$$

A_v = vertical amplitude

A_d = Diagonal amplitude, which is the distance that the diagonal spring moves

$A_{d,eq}$ = The distance the diagonal spring moves when the link ratio is factored in.

N = number of diagonal springs

K_v = K value of vertical spring

K_d = K value of diagonal spring

$$A_d = \frac{A_v}{cos\theta}$$

$$A_{d,eq} = \frac{A_d}{R}$$

$$K_{sys} = K_v + Ncos(\theta)K_d$$

2. Simulations and Results

Table 1, Properties for Original and Proposed Designs

	Original	**Design 1**	**Design 2**	**Design 3**
m	2000 kg	2000 kg	2000 kg	2000 kg
c	23892.8 kg/s	47785.6 kg/s	83624.8 kg/s	23892.8 kg/s
k	4099768.2 N/m	5124710.25 N/m	3074826.15 N/m	6149652.3 N/m
ω_n	45.275 rad/s	50.619 rad/s	39.209 rad/s	55.451 rad/s

Once we obtained our derived equation, we created code on MATLAB. In this code, we plugged in the derived equation for the steady state motion of the landing gear, along with the values that we initially calculated for the spring and damping constants. The derivation of the c, k, and ω_n values can be found in Appendix A. After obtaining the original c, k, and ω_n values, we calculated what we believed to be 3 suitable designs for the gear since they remained below .145 m at the operating frequency of the runway surface:

1. Initially, we increased and decreased the c and k values by 25% of their original value. This showed us how the landing gear behaved when each value is manipulated.
2. Upon further examination, it became clear that that increasing/decreasing k shifted the peak of the amplitude magnitude to the right/left respectively and increasing/decreasing c shifted the peak of the amplitude magnitude up/down respectively.
3. After altering the values to find out how to make the amplitude magnitude stay below .145 m at the operating frequency, 3 potential design candidates that fulfilled these criteria were created.

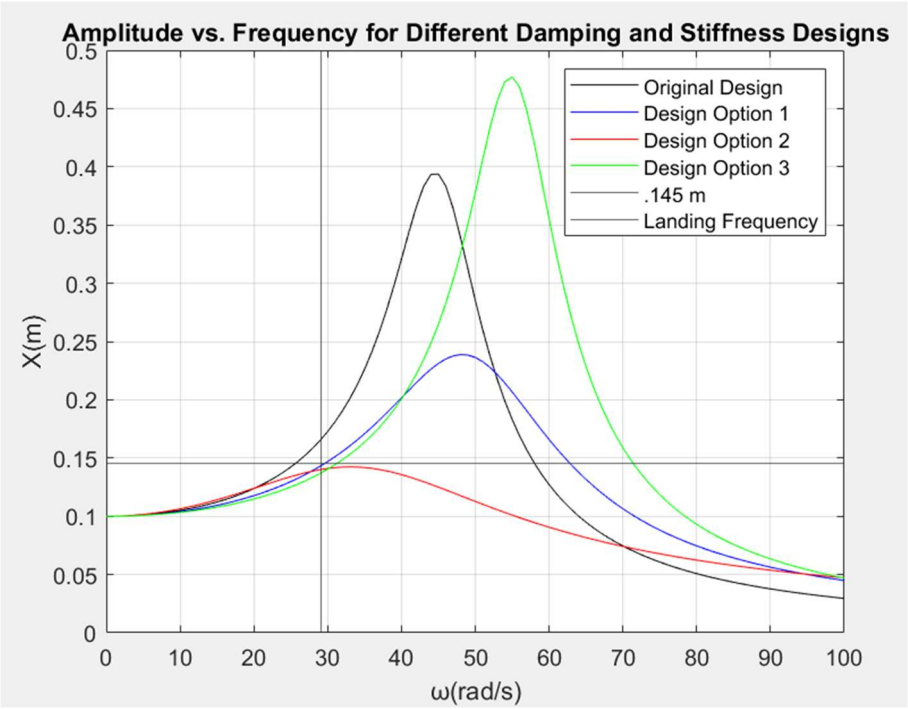

Figure 4, Amplitude vs. Frequency of the Landing Gear

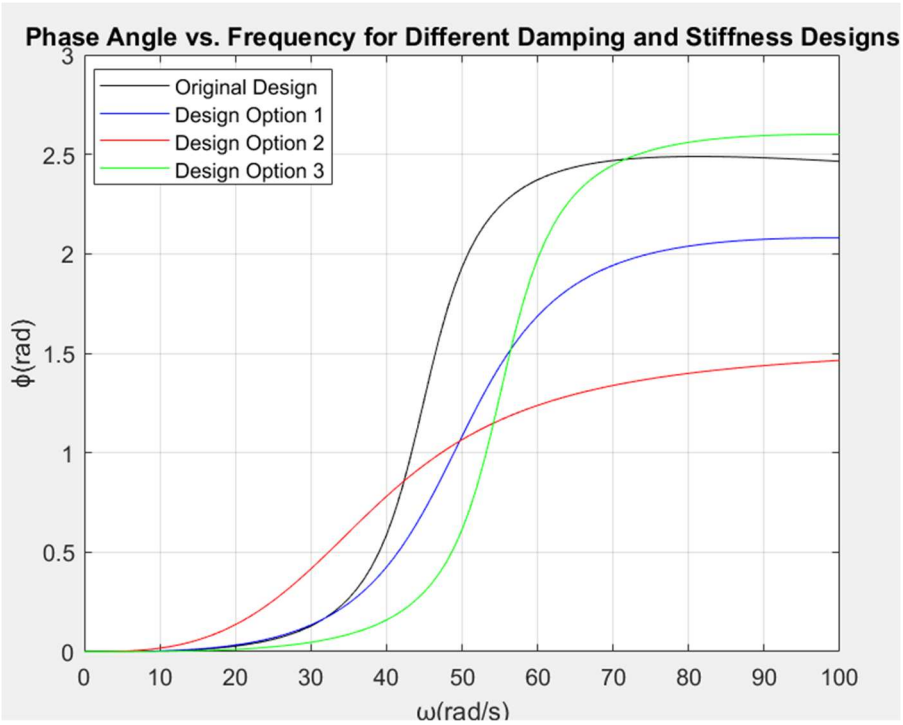

Figure 5, Phase Angle vs. Frequency of the Landing Gear

In practice, aircraft landing gear use a system called an oleo strut to provide the necessary spring/damper system to dissipate the energy transferred from the runway impacts (Figure 6). The oleo system design was patented by a British machine gun manufacturing company called Vickers Armstrong in 1915. The recoil mechanism design came from a WWI machine gun. In addition to the oleo system, the landing gear includes other trunnion braces and actuators to raise, lower and lock the landing gear in place that also provide spring and damping forces to the landing gear. The oleo system is essentially a shock absorber with two chambers, one filled with hydraulic fluid, and one filled with an inert gas like nitrogen, thar are separated by an orifice (Figure 7). A piston that is connected to the aircraft wheels is in the lower liquid filled chamber. As the wheel moves up and down, it forces hydraulic fluid through the orifice compressing nitrogen in the upper chamber. As the gas is compressed is acts like a spring absorbing the energy transferred from the wheel through the piston. Once the energy is reduced, there is a recoil action as the gas expands pushing the cylinder back down into the lower chamber. The use of nitrogen is important as this process generates heat and using an inert gas prevents the occurrence of a fire. The size of the oleo system and orifice between the upper and lower chambers is designed specifically to meet the needs of each aircraft. The oleo system provides the spring/damper system in a compact, lightweight package that allows the landing gear system to make up less than 5% of the weight of most commercial aircraft.

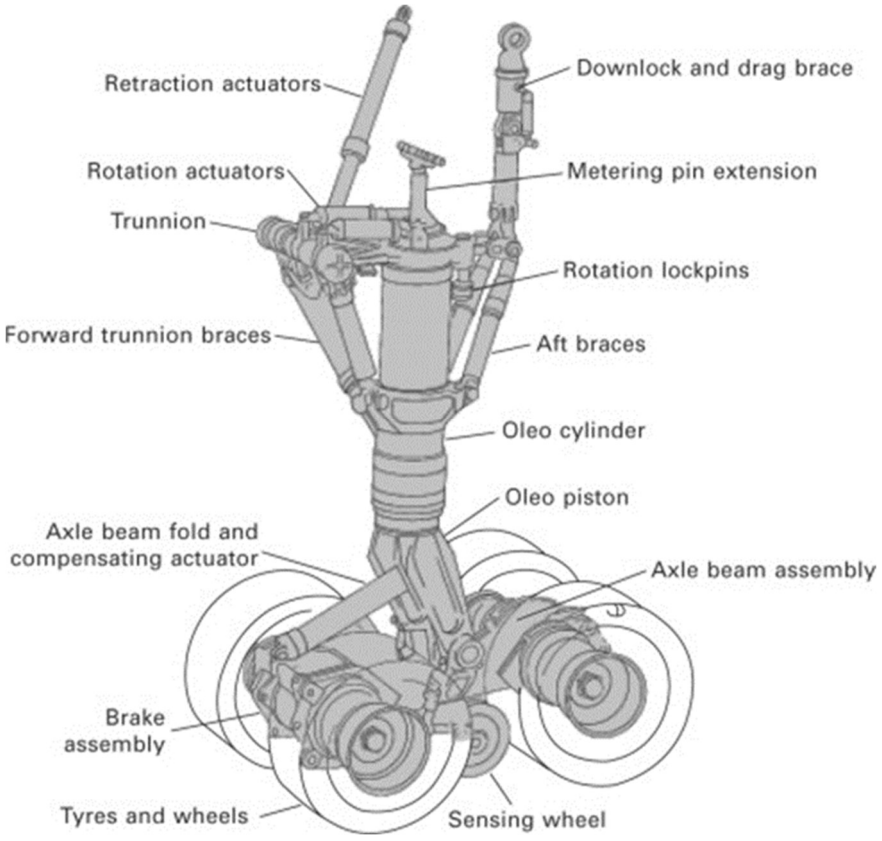

Figure 6, Typical Landing Gear Equipment including Oleo System (Mouritz, 2012)

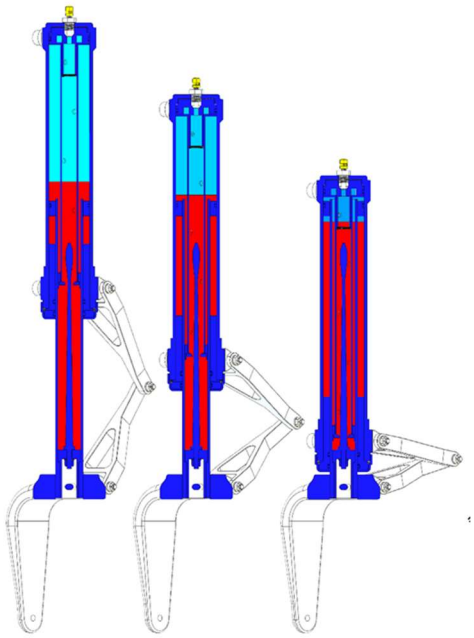

Figure 7, Oleo System showing compression of gas as piston travels upward (Olson, 2019)

For our project, we greatly simplified the design by using a combination of compression springs and linkages to mimic a central support system surrounded by trunnion braces as in Figure 5. Once we chose our 3 designs, we modelled them on an Excel file. For the basic layout, we chose to include one central spring that was positioned vertically surrounded by four that were positioned diagonally. Each diagonal spring is connected to the central vertical spring by two links with a pin connection. While the central spring would travel vertically up and down the entire range of the motion of the landing gear the ratio of the links would allow the springs on the diagonal springs to travel a much smaller distance. By reducing the travel distance, much larger k values can be achieved using compression springs. To get closer to the intended k value, we examined various combinations commercially available springs, angles of the diagonal springs, link ratios, and if necessary, the addition of more pairs of diagonal springs. Commercial springs selected for the final design choice can be found in Appendix D.

Ultimately, we chose design 2 (Figure 9), as it was the most practical option. Design 1 and design 3 were both possible to attain using commercially available springs, but they possessed characteristics that are not desirable for passenger aircraft. Since most jet aircraft have retractable undercarriage, which are housed inside the fuselage, it is preferable that they are as compact as physically possible to allow for more room. Design 1 (Figure 8), which required a link ratio of 22:1, is far wider than the other two design options, so it is likely to be more difficult to fit inside the aircraft. Design choice 3 (Figure 10), which required 6 diagonal springs instead of 4, is a more complex option, and therefore, it is likely to be less economical and heavier than design choice 1. The c-value of design choice 2, which is larger than the other two designs, means that design 2 with its higher damping constant should be preferred by passengers on the plane compared to the other two design choices. Design 2 should have less vibration cycles after bumps in the runway when compared to the other two landing gear design options.

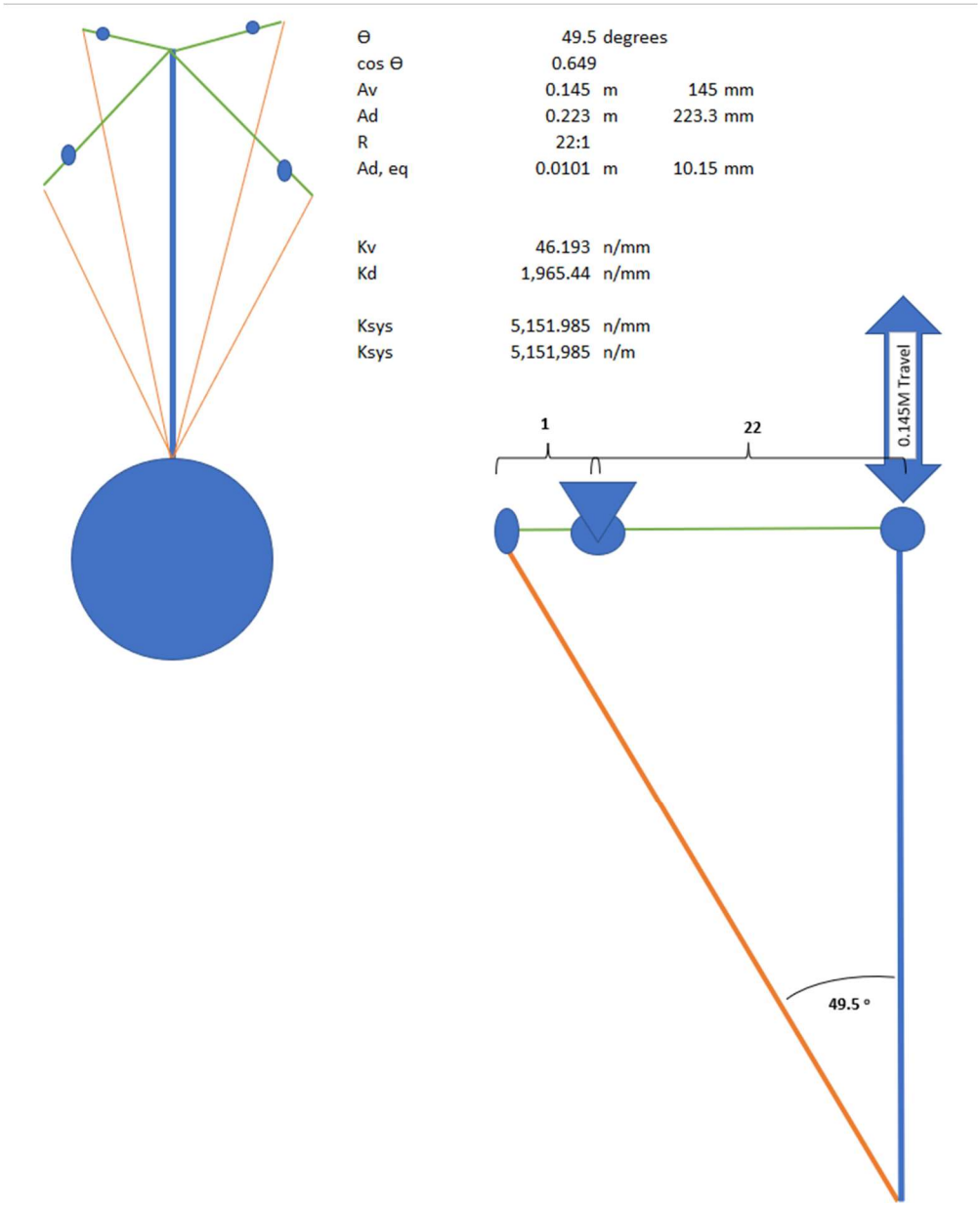

Figure 8, Diagram of Design 1 Springs

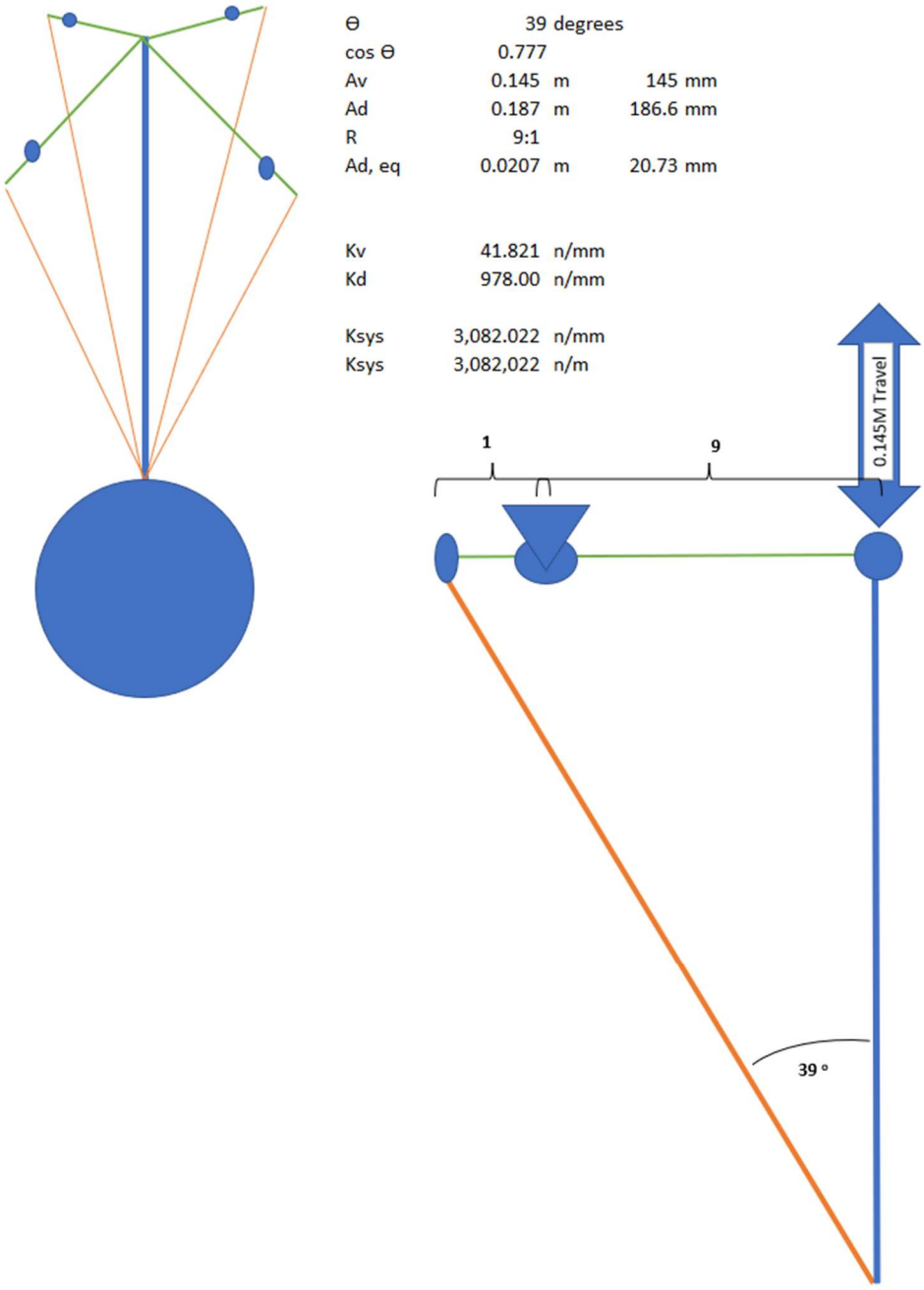

Figure 9, Diagram of Design 2 Springs

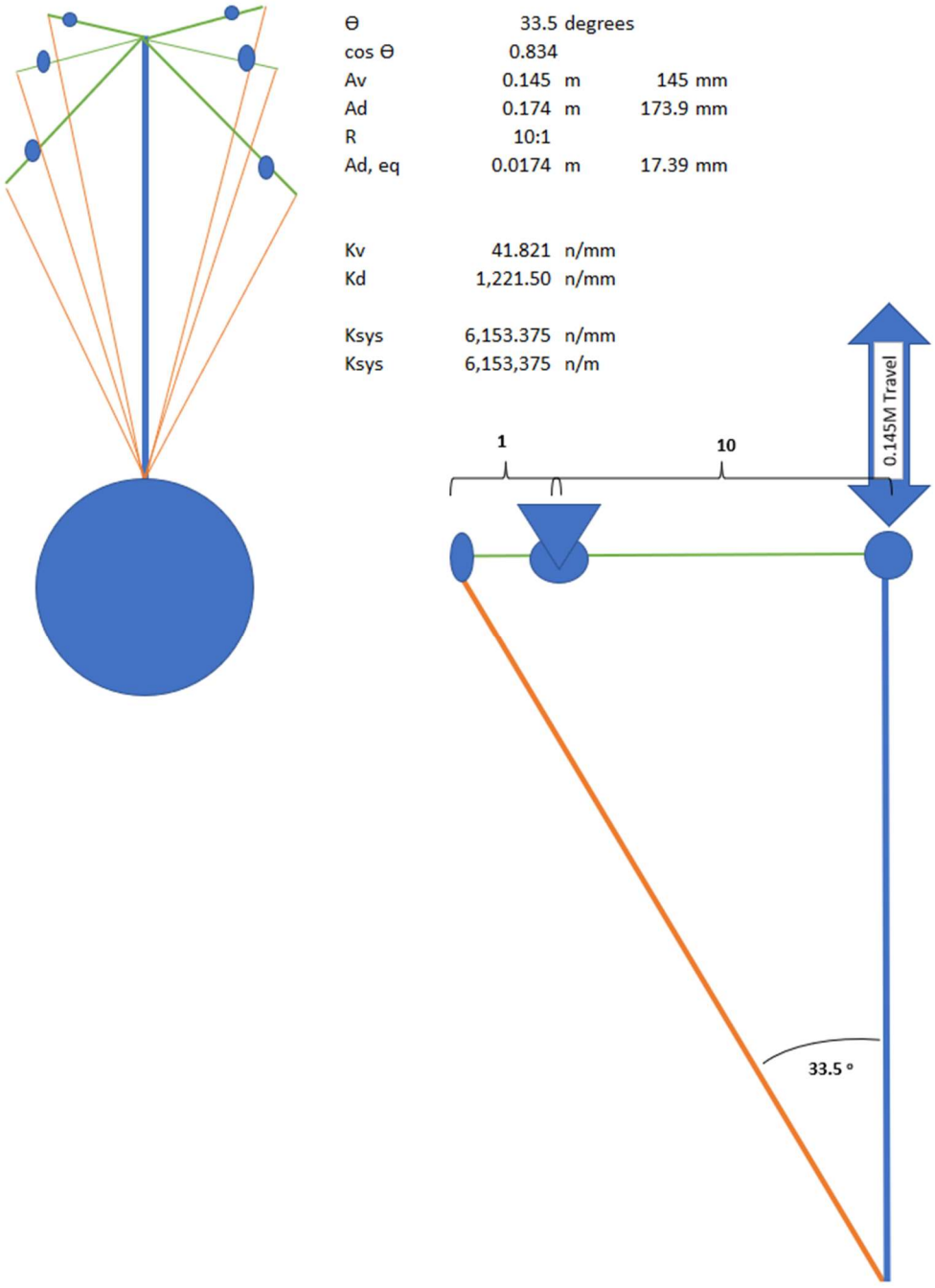

Figure 10, Diagram of Design 3 Springs

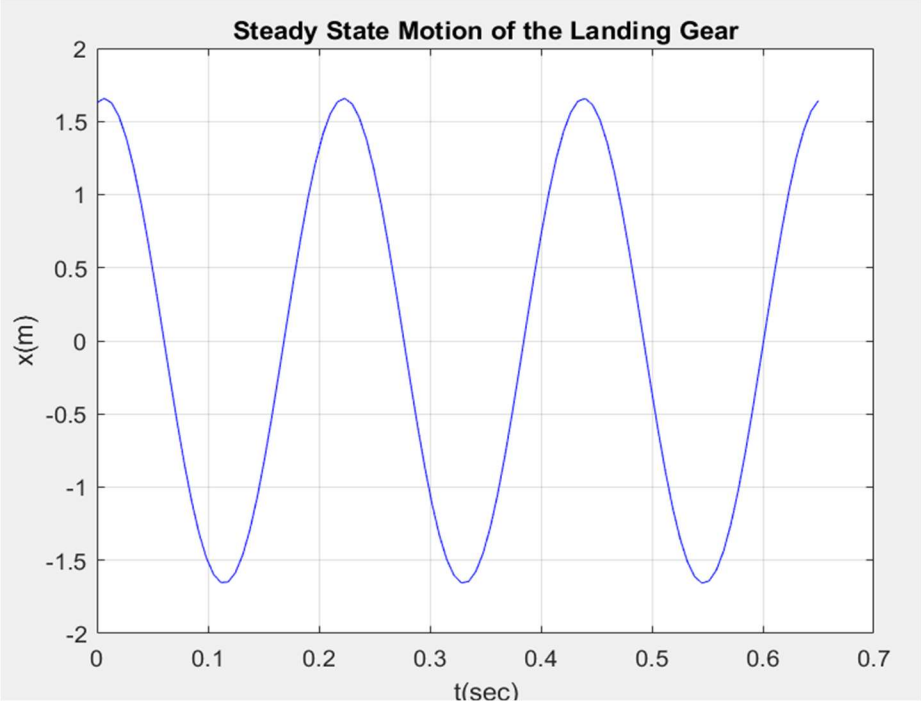

Figure 11, Steady State Motion of the Landing Gear During Takeoff and Landing

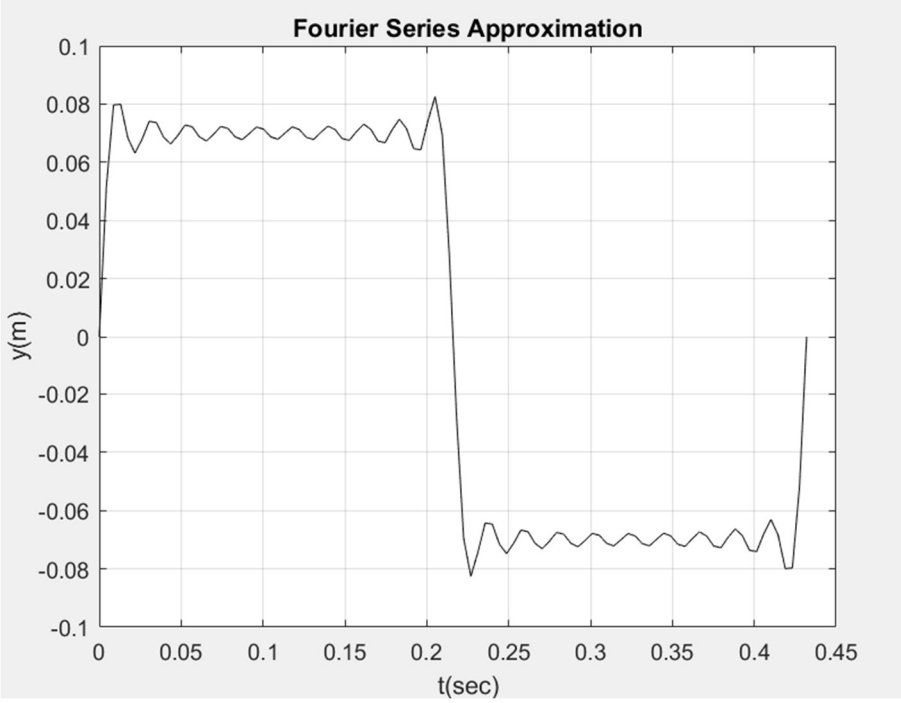

Figure 12, Plot of the Fourier Series Approximation

Square Wave Response Evaluation

When examining the interaction of a system and its surrounding forces, it is important to find the places where resonance is expected to occur. In the scenario where the external function is represented by the Fourier series approximation for the square wave, there are an infinite number of terms. However, every term does not need to be evaluated. Instead, the values should be found where $j\omega_0 \cong \omega_n$. To do this, the equation is rearranged ($j \cong \frac{\omega_n}{\omega_0}$) to find the closest possible value of j for each of the designs. The results are shown in table 2 below:

Table 2, Frequency Component Comparisons

	Original	**Design 1**	**Design 2**	**Design 3**
$\omega_{n\ (rad/s)}$	45.275	50.619	39.209	55.451
$\omega_{0\ (rad/s)}$	14.544	14.544	14.544	14.544
j	3.11	3.48	2.69	3.81

From this, the closest frequency component that would be the most likely to cause concern is j = 3 ($\omega_0 = 43.632$) . However, none of the designs fall particularly close to j = 3 except for the original one. To still check and make sure this will not be a problem, the amplitude for the j = 3 term was calculated for the original design which was the closest to the j value using the previously derived amplitude equation below:

$$|\widetilde{X_j}| = b_j \left| \sqrt{\frac{(k)^2 + (cj\omega_0)^2}{(k - m(j\omega_0)^2)^2 + (cj\omega_0)^2}} \right|$$

When the values for the original design were plugged in with the term j = 3, it was found that the amplitude of the function was about 0.116 m which is not a problem as it still falls under the max desired amplitude. Because this was the case that fell closest to resonating with the square wave and the resulting amplitude was not a problem, it reasons that this frequency component should not be a cause for concern.

3. Conclusion

The purpose of this project was to develop a working, feasible, and economically viable landing gear design that could replace a current, less practical design. After inspecting the current design, it became clear that certain alterations could improve the operation of the landing gear as the airplane approaches its landing speed. This was accomplished by improving the spring and damper of the landing gear by observing how different springs and dampers behaved under the same conditions. One technique that was used at this point in the project was to hold the damper value constant and change the spring's value until a sufficient outcome was achieved and then change the damper value, while the spring value remained the same, until the landing gear reached the following outcome. If the magnitude of the amplitude fell under the selected value of .145 m at the frequency of the landing gear as the airplane lands, the designs passed the first test. These designs were then tested based on the conditions listed above such as feasibility,

customer value, and more. The design that was selected easily falls under the amplitude magnitude and will be very straight forward to replicate physically. Since this design has spring and damping values very close to that of the original design, there will not be any issues with technological limitations that would make the design nearly impossible to achieve.

The work done on this project will be extremely useful in any future projects that deal with the altering of the landing gear of an airplane. Although the work done in this project is specific to the original landing gear design and the 3 designs that successfully fit the necessary criteria of the runway landing, this process can be used to find out how landing gear operates on a landing surface different than the one this project used. It will be possible to see if and where a landing gear design will run into problems while it travels over unforeseen landing surfaces.

4. Appendix A

Logarithmic Decrement of the Original Landing Gear Motion

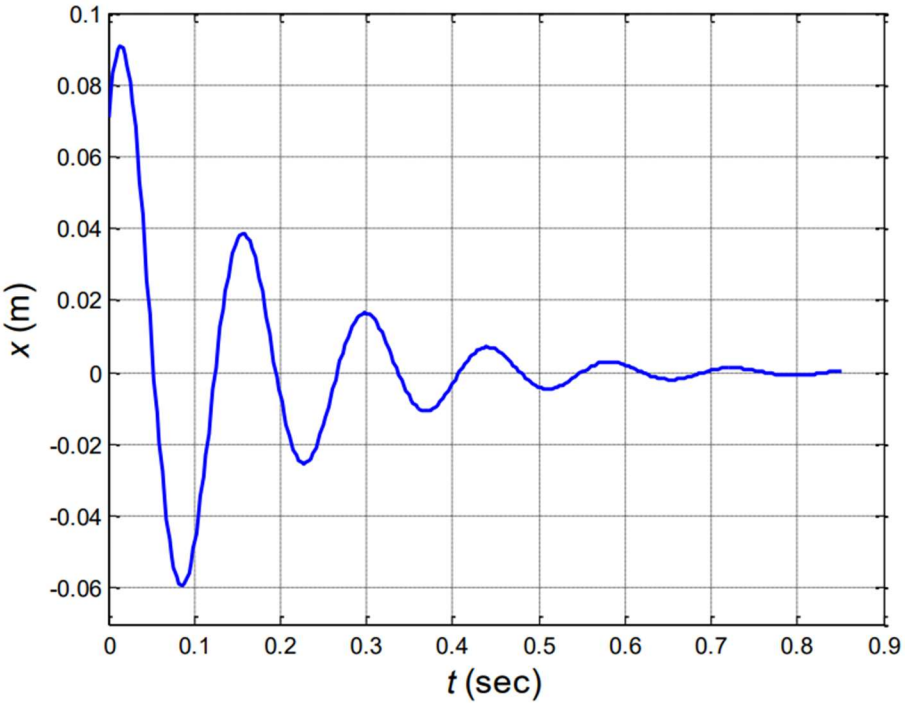

Figure 7, Logarithmic Decrement Given

From this image of the transient motion, it is estimated that the first peak of the logarithmic decrement x_1 occurs around .09 m and the second x_2 occurs at .039 m. The time constant τ_d (the distance between the peaks on the logarithmic decrement) is about .14 sec.

Using the logarithmic decrement (δ) equation:

$$\delta = ln\left(\frac{x_1}{x_2}\right) = ln\left(\frac{.09\ m}{.039\ m}\right) = .836$$

Next, using the damping ratio (ζ) equation:

$$\zeta = \frac{\delta}{\sqrt{(2\pi)^2 + (\delta)^2}} = \frac{(.836)}{\sqrt{(2\pi)^2 + (.836)^2}} = .1319$$

Now there is enough information to solve for the natural frequency (ω_n):

$$\omega_n = \frac{\delta}{(\zeta)(\tau_d)} = \frac{.836}{(.1319)(.14\ sec)} = 45.28\ {}^{rad}/_{sec}$$

Using the natural frequency, solve for the spring constant (k) and damping constant (c) values for the original landing gear system:

$$\omega_n = \sqrt{\frac{k}{m}}$$

$$k = (\omega_n)^2(m) = (45.28\ {}^{rad}/_{sec})^2(2000\ kg) = 4099768.2\ {}^{N}/_{m}$$

$$2\,\zeta\omega_n = \frac{c}{m}$$

$$c = 2\,\zeta\omega_n m = 2(.1319)(45.28\ {}^{rad}/_{sec})(2000\ kg) = 23892.8\ {}^{kg}/_{s}$$

5. Appendix B

Derivation of the particular solution

From the free body diagram, Newtons 2nd Law can be used to derive the Equations of Motion (EOM).

$$\sum F_y = m\ddot{x}$$

$$-c(\dot{x} - \dot{y}) - k(x - y) = m\ddot{x}$$

After rearranging the terms related to the system on the left and the terms related to the external forces on the right, the EOM takes the form of:

$$m\ddot{x} + c\dot{x} + kx = c\dot{y} + ky$$

The given equation for the forcing function is: $y(t) = Y_0 \cos(\omega t)$ where Y_0 is the amplitude, ω is the forcing frequency, and t is the time

But for now, assume $y(t) = Y_0 e^{i\omega t}$ and $\dot{y}(t) = i\omega Y_0 e^{i\omega t}$

Plugging $\dot{y}$ and y into the EOM and rearranging to group the common exponential term:

$$m\ddot{x} + c\dot{x} + kx = c(i\omega Y_0 e^{i\omega t}) + k(Y_0 e^{i\omega t})$$

$$m\ddot{x} + c\dot{x} + kx = Y_0(k + ic\omega)e^{i\omega t}$$

To simplify, call $\tilde{Y} = Y_0(k + ic\omega)$

Assume particular solution and velocity and acceleration derivatives:

$$x_p(t) = \tilde{X}e^{i\omega t},\ \dot{x_p}(t) = i\omega\tilde{X}e^{i\omega t},\ \ddot{x_p}(t) = -\omega^2\tilde{X}e^{i\omega t}$$

Now plugging the particular solution into the equation of motion and rearranging to group the common exponential term this becomes:

$$m\left(-\omega^2\tilde{X}e^{i\omega t}\right) + c\left(i\omega\tilde{X}e^{i\omega t}\right) + k\left(\tilde{X}e^{i\omega t}\right) = \tilde{Y}e^{i\omega t}$$

$$[(k - m\omega^2) + ic\omega]\tilde{X}e^{i\omega t} = \tilde{Y}e^{i\omega t}$$

Because the left and right side of the equations take on a similar form, the constants in front of the exponential term can be equated and used to solve for $\tilde{X}$.

$$\tilde{X} = \frac{\tilde{Y}}{[(k - m\omega^2) + ic\omega]}$$

Plugging $\tilde{X}$ and $\tilde{Y}$ back into the assumed particular solution:

$$x_p(t) = \frac{Y_0(k + ic\omega)}{[(k - m\omega^2) + ic\omega]}e^{i\omega t}$$

To write this equation in a non-complex manner, the terms are converted into polar form:

$$x_p(t) = Y_0\left|\sqrt{\frac{(k)^2 + (c\omega)^2}{(k - m\omega^2)^2 + (c\omega)^2}}\right|\frac{e^{i\phi_1}}{e^{i\phi_2}}e^{i\omega t}$$

After rearranging the exponential terms and combining the 2 phase angles into a single value

$\phi = \phi_2 - \phi_1$, the particular solution can now be written in its final form:

$$x_p(t) = \left|\tilde{X}\right|e^{i(\omega t - \phi)} \text{ where } \left|\tilde{X}\right| \text{ and } \phi \text{ are given by}$$

$$\left|\tilde{X}\right| = Y_0\left|\sqrt{\frac{(k)^2 + (c\omega)^2}{(k - m\omega^2)^2 + (c\omega)^2}}\right|$$

$$\phi = \tan^{-1}\frac{cm\omega^3}{k(k - m\omega^2) + (c\omega)^2}$$

6. Appendix C

Fourier Series Approximation Derivation for Square Wave

Figure 8 represents the shape of a stretch of ground and is said to continue for 6 cycles.

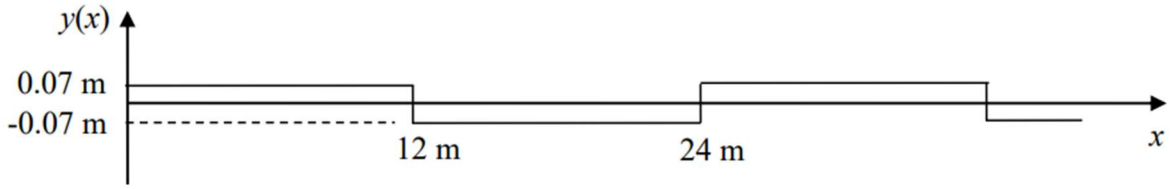

Figure 8, Unforeseen Motion of the Base as a Function of x

Because the square wave graph shown above is originally given in terms of x distance vs. y displacement, these terms must first be translated into a time dependent graph. This can be done using the given velocity and wavelength obtained from the graph to calculate the function frequency.

$$\tau = \frac{\lambda}{v}$$

Where τ is the period of the function in (s), λ is the wavelength in (m) obtained from the given graph figure 8 and v is the velocity of the examined landing gear in (m/s). From this, a function for the new parameterization can now be obtained which is shown in figure 9. Only the first cycle will be examined using the Fourier Series Approximation, but the same equation can be applied to the next 5 cycles of repetitive motion. The square wave can be written using a piecewise function to break each cycle into two parts:

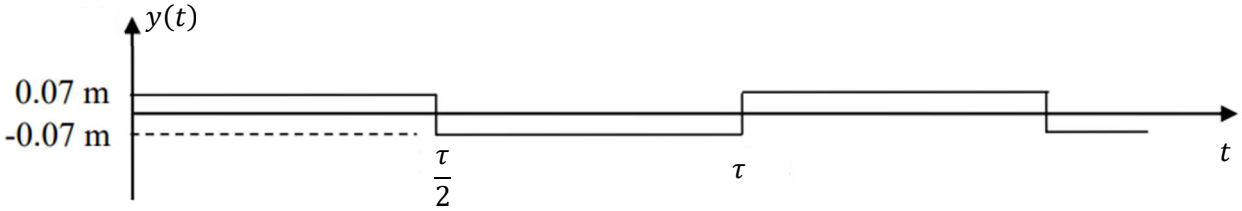

Figure 9, Unforeseen Motion of the Base as a Function of t

$$\begin{cases} f(t) = A & for\ 0 < t < \frac{\tau}{2} \\ f(t) = -A & for\ \frac{\tau}{2} < t < \tau \end{cases}$$

Where A is the amplitude of the wave in (m), t is time in (s), and τ is the period found above. Next, the fundamental frequency (ω_0 in rad/s) can be calculated again using the period found above:

$$\omega_0 = \frac{2\pi}{\tau}$$

The Fourier Series is written in the form:

$$y(t) \cong \frac{a_0}{2} + \sum_{j=1}^{\infty} a_j \cos j\omega_0 t + b_j \sin j\omega_0 t$$

Where a_0, a_j, b_j are all harmonics derived with respect to the given function and j is an integer. The derivation of b_j is as follows:

$$b_j = \frac{2}{\tau}\int_0^{\tau} f(t) \sin j\omega_0 t \, dt$$

The integral can be broken into two parts to accommodate the piecewise function f(t) and bounds set accordingly.

$$b_j = \frac{2}{\tau}\left[\int_0^{\frac{\tau}{2}} A \sin j\omega_0 t \, dt + \int_{\frac{\tau}{2}}^{\tau} -A \sin j\omega_0 t \, dt\right]$$

Now this function can be integrated and rearranged to simplify.

$$b_j = \frac{2}{\tau}\left[\left[-\frac{A}{j\omega_0}\cos j\omega_0 t\right]_0^{\frac{\tau}{2}} - \left[-\frac{A}{j\omega_0}\cos j\omega_0 t\right]_{\frac{\tau}{2}}^{\tau}\right]$$

$$b_j = \frac{2}{\tau} * \frac{A}{j\omega_0}\left[\left(-\cos j\omega_0 \frac{\tau}{2} + \cos 0\right) + \left(\cos j\omega_0 \tau - \cos j\omega_0 \frac{\tau}{2}\right)\right]$$

Plugging in $\omega_0 = \frac{2\pi}{\tau}$ to this equation and combing terms this becomes:

$$b_j = \frac{A}{j\pi}[\cos 2j\pi - 2\cos j\pi + 1]$$

Because of the nature of the cosine function, different results will be obtained when using even and odd numbers. To see this phenomenon, two different cases will be examined. First, plugging in an odd multiple of j:

$$b_3 = \frac{A}{3\pi}(\cos 6\pi - 2\cos 3\pi + 1) = \frac{A}{\pi}(1 - 2(-1) + 1) = \frac{4A}{3\pi}$$

From this, it is found that for any odd value of j, $b_j = \frac{4A}{j\pi}$. Now substituting in an even value for j:

$$b_3 = \frac{A}{2\pi}(\cos 4\pi - 2\cos 2\pi + 1) = \frac{A}{\pi}(1 - 2(1) + 1) = 0$$

Thus, for any even value of j, b_j will wind up being equal to zero. The equations for calculating a_0 and a_j follow a similar form and are shown below.

$$a_0 = \frac{2}{\tau}\int_0^{\tau} f(t)dt$$

$$a_j = \frac{2}{\tau}\int_0^{\tau} f(t)\cos j\omega_0 t\, dt$$

After following the same method to derive a_0 and a_j, it is found that $a_0 = 0$ and $a_j = 0$Therefore, when substituting all constants back into the original form of the Fourier Series, the only contributing term is the sine component and within that, only odd values of j must be examined. Written out, this approximation of the square wave function takes the form of:

$$y(t) \cong \sum_{j=1,3,5}^{\infty} \frac{4A}{j\pi}\sin j\omega_0 t$$

7. Appendix D

Springs used for design 2

THE SPRING STORE
By ACXESS SPRING

sales@thespringstore.com Ph 951 276 2777
2225 E. Cooley Dr Colton, CA 92324
www.thespringstore.com

Part Name:	Date: 03/20/2022
Part #: in	PC1000-4500-8000-HD-10500-CG-N-IN
Part #: mm	PC25400-114300-8000-HD-266700-CG-N-MM
Spring Type: Compression Spring	End Type: Closed & Ground
Finish: None	Direction of Wind: Right Hand
Material: Hard Drawn ASTM A227	Spring Index (I): 3.5
Weight / M: 19630.5253 Lbs	Length of W: 87.9646 in

Physical Dimensions	IN	MM	Tolerances (in)
Wire Diameter (WD)	1.000 in	[25.400 mm]	+/- 0.0017
Outer Diameter (OD)	4.500 in	[114.300 mm]	+/- 0.19
Inner Diameter (ID)	2.500 in	[63.500 mm]	+/- 0.19
Free Length (FL)	10.500 in	[266.700 mm]	+/- 0.4
Active Coils (AC)	6.000	[6.000]	+/- 1/4 coil
Total Coils (TC)	8.000	[8.000]	+/- 1/4 coil
Solid Height (SH)	8.000 in	[203.200 mm]	+/- 0.56

Spring Rate (K)	5584.534 lbs/in	978.002 N/mm	+/- 558.4534
Max Load (ML)	5067.149 lbf	2298.420 kgs	+/- 506.71487
Max Travel (MT)	0.907 in	23.048 mm	

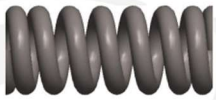

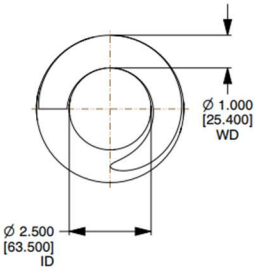

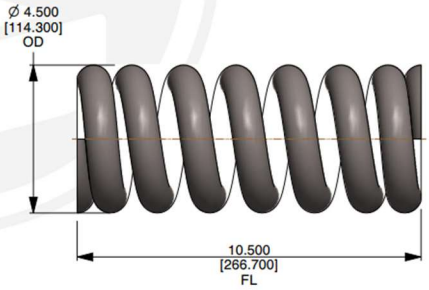

Notes

Scale: 0.262

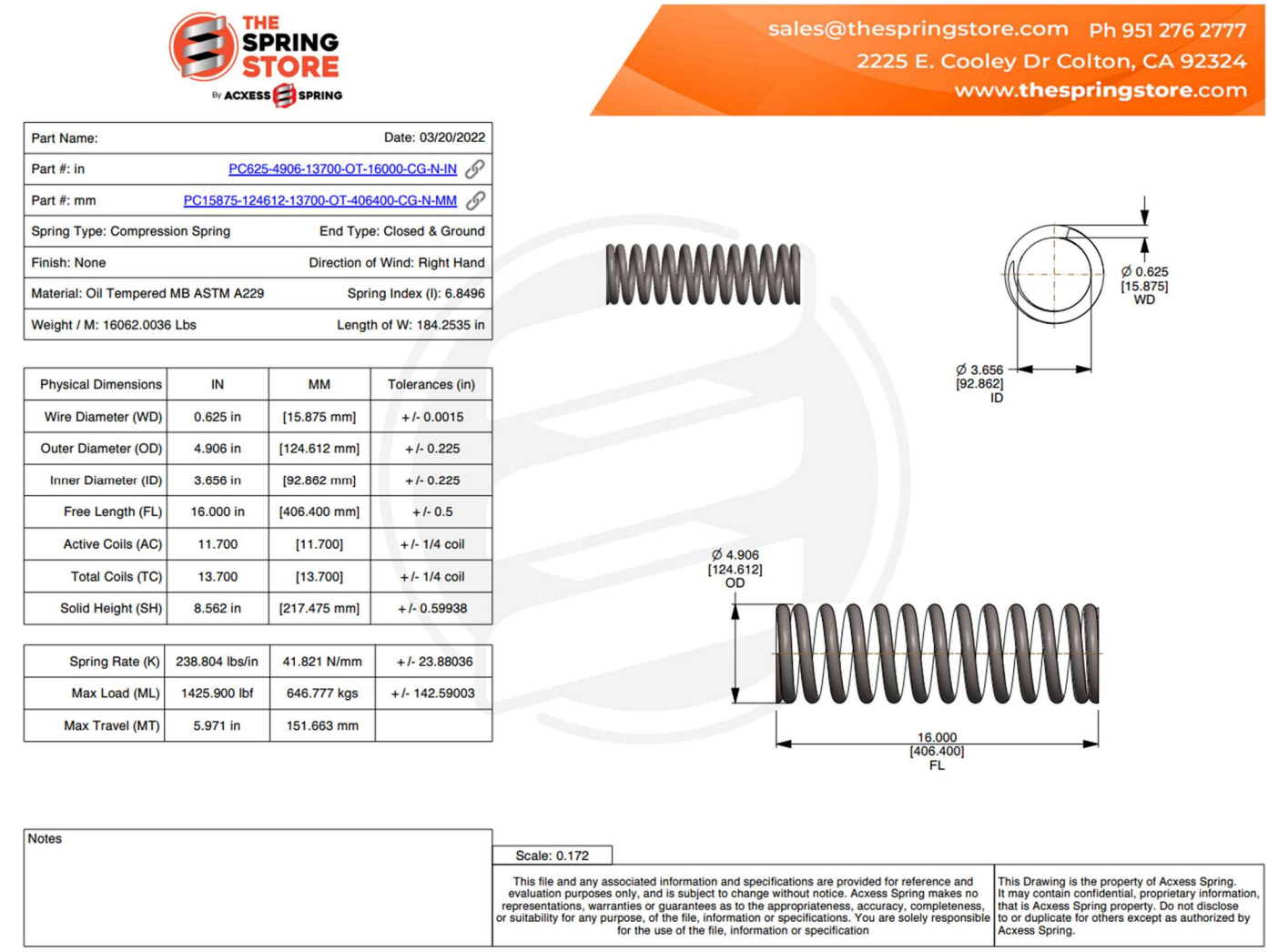

8. Bibliography

A. P. Mouritz, "Landing Gear," *Landing Gear - an overview | ScienceDirect Topics*, 2012. [Online]. Available: https://www.sciencedirect.com/topics/engineering/landing-gear. [Accessed: 22-Mar-2022].

E. Olson, "How do oleo-pneumatic shock struts work?," *How do oleo-pneumatic shock struts work? | Engineering360*, 07-Nov-2019. [Online]. Available: https://insights.globalspec.com/article/12954/how-do-oleo-pneumatic-shock-struts-work#:~:text=Oleo%20struts%20are%20critical%20elements,the%20ground%20to%20the%20airframe. [Accessed: 22-Mar-2022].